



Special Issue: Near Infrared Spectroscopy of Soil

Technical note:

Characterisation of loess soils using near infrared photoacoustic spectroscopy

Du Changwen,* Ma Fei, Shen Yazhen and Zhou Jianmin

The State Key Laboratory of Soil and Sustainable Agriculture, Institute of Soil Science, Chinese Academy of Sciences, Nanjing 210008, PR China. E-mail: chwdu@issas.ac.cn

The photoacoustic spectroscopy (PAS) technique has emerged as a valuable tool for the study of soil materials. The present work developed the experimental set-up for near infrared (800–2400 nm) photoacoustic spectroscopy (NIR-PAS), which consists of photoacoustic (PA) accessory, tungsten bromine lamp, monochromator, chopper and lock-in-amplifier, and this spectrometer was first applied to record the spectra of soils ($n = 50$) collected from the Loess Plateau of China; partial least-squares regression (PLSR) models and leave-one-out cross-validation were used to predict soil organic matter (SOM), clay, carbonate and available phosphorus content. The spectra varied among different soil samples; SOM played an important role in the spectral appearance, and the intensity and position of five typical absorption bands significantly shifted owing to the variances in the components and structure of SOM. The PLSR model demonstrated a good performance in the prediction of SOM with a root mean square error of 2.5 kg kg^{-1} and a ratio of standard deviation to prediction error of 2.3. This pilot study demonstrates that NIR-PAS exhibits typical infrared absorptions and may be suitable for analysing soil samples.

Keywords: loess soil, soil organic matter, near infrared photoacoustic spectroscopy, combinational and overtone bands, chemometrics

Introduction

Near infrared spectroscopy (0.8–2.5 μm , i.e. 12,500–4000 cm^{-1}) has been widely used for soil proximal sensing owing to the advantages in terms of cost and portability of the instruments.^{1,2} Over the last 30 years, photoacoustic spectroscopy (PAS) has attracted the attention of researchers.^{3–6} These methods emerged as valuable tools for optical and thermal characterisation of a wide range of samples offering significant improvements (high sensitivity and precision) over traditional methods. PAS is based on the principle of detection of non-radiative relaxation energy, resulting when molecules of the sample are excited from the ground state to higher energy states, by a periodic absorption of radiation. Non-radiative relaxation processes (such as collisions with other molecules) lead to local warming of the sample matrix; pressure fluctua-

tions are then generated by thermal expansion, which can be detected by a very sensitive microphone. The resulting spectrum differs from both equivalent transmittance and reflectance spectra, since the technique detects non-radiative transitions in the sample. The suitability of the PAS technique lies in the fact that it can be applied irrespective of the physical state of the samples (including solid and gas samples). It is a non-destructive technique that can be applied in opaque, transparent and highly scattering samples such as biological, chemical and even geological samples and possibly soils.^{7–9} Specific portable and cheap PAS instrumentation for gas sampling has come into use,¹⁰ thereby potentially leading to rapid fast soil analysis; thus, the objective of this pilot study is to explore the feasibility of NIR-PAS in soil analysis.

Materials and methods

Soil samples ($n = 50$) were randomly collected from agricultural fields located at the Loess Plateau of China (Figure 1) at a depth of 0–20 cm. Upon returning from the field, samples were air-dried at room temperature and passed through a 2 mm sieve. Soil organic matter (SOM), clay, carbonate content and available P (Olsen P) were determined using routine methods:^{11–12} the potassium dichromate method was used for SOM determination, the wet disperse method for clay determination and the gasometric method for carbonate determination, and Olsen P was extracted by NaHCO_3 . The measured values of these parameters are shown in Table 1.

Spectrometer set-up

A schematic diagram of the experimental set-up used in the present study is shown in Figure 2. Helium was used to purge the PA cell, and nitrogen gas was used to remove the vapour and CO_2 in the instrument. The near infrared range of 800–2400 nm was involved; carbon black was used to optimise the chopping frequency and was used as reference in the spectra scan of soil samples with a resolution of 8 nm.

Reflectance NIR spectra were also recorded (FieldSpec® Pro, ASDI, Boulder, CO), and the wavelength range was in the

range of 800–2400 nm with a resolution of 4 nm. Thirty-two scans were taken and averaged.

Data processing

Spectra (NIRS spectra and PAS spectra) were preprocessed with a smoothing filter (first-order Savitzky–Golay filter with a 23-point window).¹³ The filtered spectra were then normalised for use, and the functions of “mapstd” and “filtfilt” in software Matlab 7.8 (Mathworks, Natick, MA) was used to smooth and normalise the spectra data, which were used for statistical analyses described below.

A quantitative analysis of the NIRS spectra and PAS spectra was performed using partial least-squares regression (PLSR). The detailed PLSR algorithm used in the analysis was well described by Geladi and Kowalski.¹⁴ Leave-one-out cross-validation was conducted in the prediction. The number of PLSR factors was optimised by increasing the number of components to the point where the validation error (root mean square error, RMSE) and determination coefficient did not change substantially with further increases in PLSR factors.⁸

$$RMSE = \sqrt{\frac{\sum (y - y')^2}{n}} \quad (1)$$

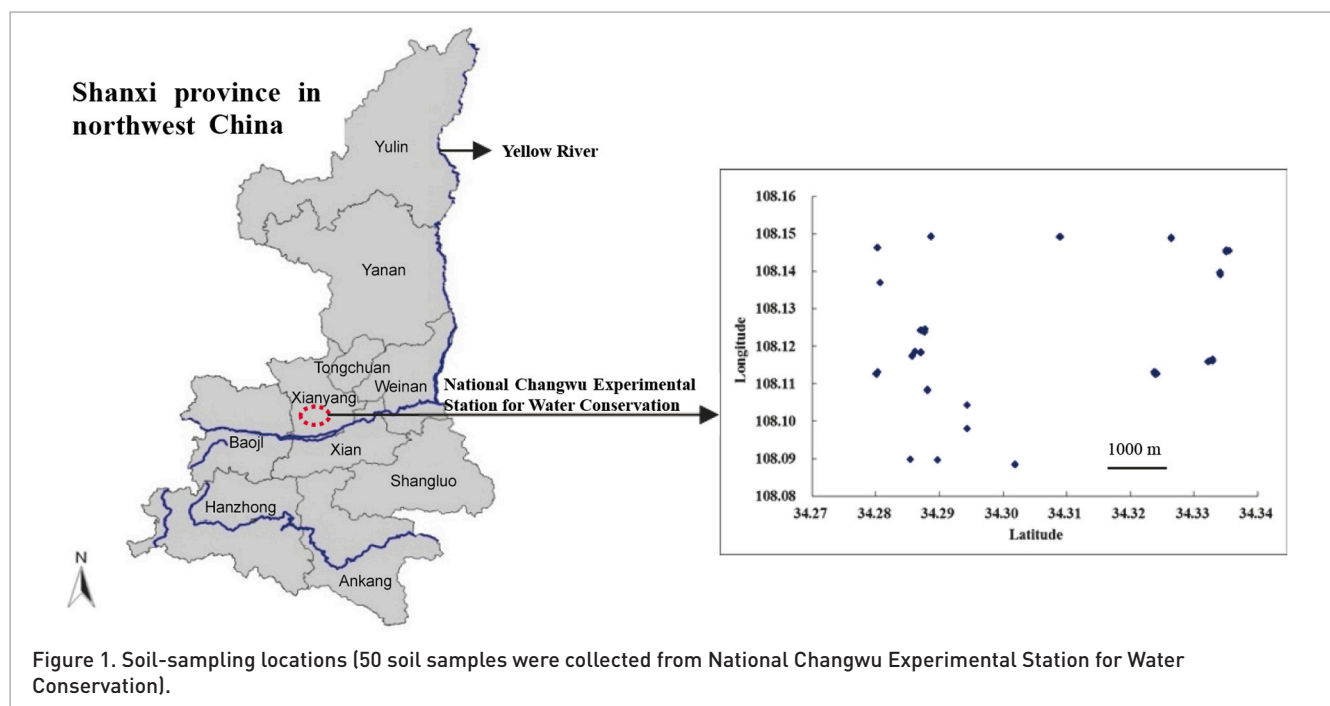


Figure 1. Soil-sampling locations (50 soil samples were collected from National Changwu Experimental Station for Water Conservation).

Table 1. Sample mean and range of selected soil properties ($n = 50$).

	Organic matter (g kg^{-1})	Clay (%)	Carbonate (%)	Olsen P (mg kg^{-1})
Mean	17.4	13.0	9.2	81
Maximum	28.6	15.8	12.9	219
Minimum	7.2	9.6	4.3	5.2
SD	4.1	1.7	1.6	46

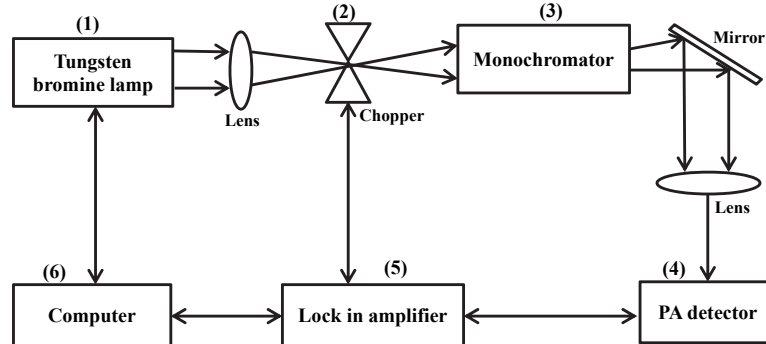


Figure 2. Schematic diagram of photoacoustic spectrometer. (1) LHT150 QTH, Zolix, China; (2) model SR-540, Stanford, USA; (3) Omni- λ 150, Zolix, China; (4) Model 300, METC, USA; (5) model SR-810, Stanford USA; (6) software from Zolixscan, Zolix, China.

where y and y' denote the predicted and actual values, respectively, and n is the number of soil samples.

Bias was calculated as:

$$\text{Bias} = \sqrt{\frac{\sum(\bar{y} - y')^2}{n}} \quad (2)$$

where \bar{y} and y' denote the mean of predicted value and actual value, respectively, and n is the number of soil samples.

The ratio of standard deviation of each soil parameter to prediction error (RPD) was also calculated to confirm the optimised PLS factors:

$$RPD = SD / RMSEV \quad (3)$$

where SD is the standard deviation in calibration set, and $RMSEV$ is the root mean standard error ($RMSE$) in cross-validation.

IQ is a parameter to express deviation instead of SD for a sample set with non-Gaussian distribution and was calculated as:

$$IQ = Q_3 - Q_1 \quad (4)$$

where Q_1 refers to the value below which 25% of the samples are included, and Q_3 refers to the value below which 75% of the samples are included.

$RPIQ$ was then calculated as a similar parameter of RPD to evaluate the model performance:¹⁵

$$RPIQ = IQ / RMSEV \quad (5)$$

Matlab 7.8 software was used to analyse the spectral data.

Results and discussion

Variation of PA signal with chopping frequency

In general, the PA signal decreased with increasing chopping frequency; the intensity of the PA signal was strongest at around 900 nm and then significantly decreased with the increase in wavelength; and the PA signal was very weak when the wavelength was higher than 2000 nm.

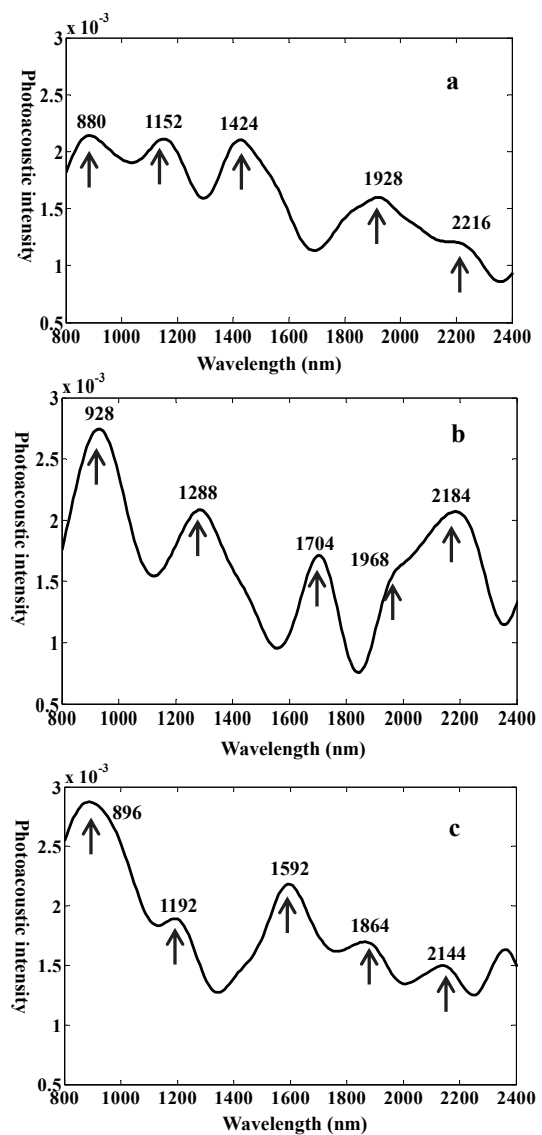


Figure 3. Near infrared photoacoustic spectra of loess soils (typical bands and position were indicated). (a) Loess soil with low organic matter content (0.72%); (b) loess soil with median organic matter content (1.53%); (c) loess soil with high organic matter content (2.89%).

Table 2. Tabulated infrared bands assigned to molecular structure in the near infrared range (800–2400 nm).

Wavelength (nm)	Assignment	References
880, 896, 928	O–H third overtone	17, 18
1152, 1192	N–H second overtone	19, 20
1288	C–H second overtone	18, 19, 21
1424	O–H first overtone	17, 19, 21
1592	N–H first overtone	19, 21
1704	C–H first overtone	18, 19, 21
1864	O–H combination	17, 19, 21
1928	N–H combination	19, 21
1968	C–H combination	17, 20
2144, 2184, 2216	C–O combination	18, 20

The PA signal was inversely proportional to the frequency in the range 10–40 Hz, but the variation of PA signal was not the same, and the PA signal decreased faster at a high frequency (this has been verified for an optically opaque solid).¹⁶

Though the PA signal intensity was high in the low chopping frequency, the signal was noisier while it was smoother at a higher chopping frequency. The signal-to-noise ratios were around 6.2, 10.5, 9.3 and 8.9 for the chopping frequencies of 10 Hz, 20 Hz, 30 Hz and 40 Hz, respectively. Therefore, 20 Hz was selected to record the soil spectra used in the followed characterisation.

NIR-PAS spectra of loess soils

The NIR-PAS spectra (800–2400 nm) of loess soils are shown in Figure 3; five bands can be clearly observed in the spectra for the loess soils.

The assignments of absorption bands are indicated in Table 2, mainly appearing as O–H, N–H, C–H and C–O overtone and combinational vibrations. The bands of metal oxides are usually located at less than 800 nm, and the bands of some

other clay minerals, such as carbonate and smectite, are located at 2000–2400 nm.^{17–21} Theoretically, these vibration bands can be used to qualify the SOM content. However, some of these bands are not applicable for estimating carbonate content because of the weak absorption intensity and/or interfering vibrations associated with other soil components (e.g. soil carbonate and soil mineral clay) (Table 1). Therefore, a multivariate data analysis is required to extract hidden information in the infrared spectra.

PLSR modelling of soil parameters

The statistics results associated with PLSR modelling for SOM based on total spectral range are shown in Figure 4. Better prediction performances were obtained, followed by Olsen P (Table 3), while the predictions were relatively poor for clay; the predictions using NIR-PAS were the same as or slightly better than that using reflectance NIRS. Therefore, NIR-PAS indicated the potential of soil analysis as an alternative technique.

The distribution of SOM in the soils studied ($n = 50$) deviates greatly from a normal distribution curve. Therefore, a more robust index, *RPIQ* instead of *RPD* calculation, was suggested by Bellon-Maurel *et al.*¹⁵ Calculations of this metric may be more reasonable for soil science applications and are included in Table 3.

Although a satisfactory prediction was obtained using the NIR-PAS technique in this pilot study, since knowledge about the application of NIR-PAS in soil analysis is very limited much more effort should be made as regards NIR-PAS spectra acquisition as well as spectral data analysis (data mining). For the spectral acquisition, the NIR-PAS instrumental set-up and spectra scanning parameters need to be further optimised, so that spectra with more abundant soil information as well as less subjective and systematic interferences can be recorded; for the spectral data analysis, more soil samples and soil types, soil properties as well as suitable chemometric tools should be involved in the pretreatment (filter, normalisation,

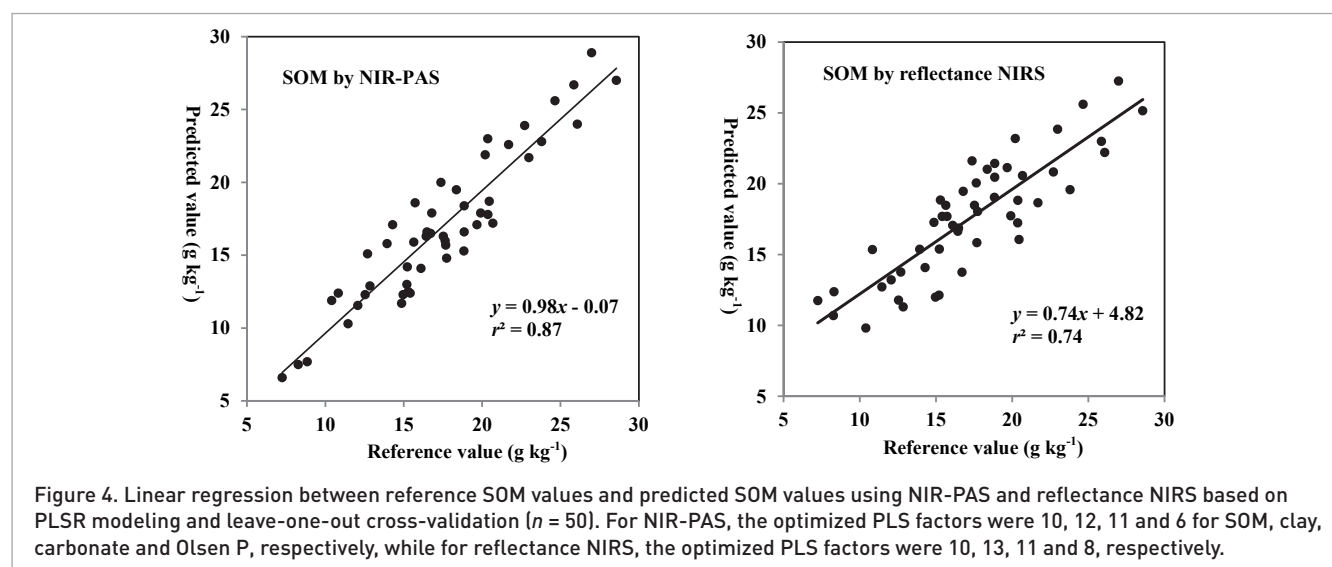


Table 3. Statistics of model performance for predicting selected soil properties using NIR-PAS and reflectance NIRS.

Spectroscopy method	Soil property	RMSECV	Bias	r^2	RPD	RPIQ
NIR-PAS	SOM (g kg^{-1})	2.5	0.50	0.87	2.3	3.0
	Clay (%)	1.1	0.22	0.52	1.5	1.6
	Carbonate (%)	0.9	0.18	0.71	1.8	2.0
	Olsen-P (mg kg^{-1})	25	0.61	0.71	1.9	2.2
Reflectance NIRS	SOM (g kg^{-1})	2.8	0.51	0.74	2.0	2.8
	Clay (%)	1.1	0.18	0.55	1.5	1.6
	Carbonate (%)	0.9	0.08	0.65	1.7	1.9
	Olsen-P (mg kg^{-1})	29	0.81	0.60	1.6	1.8

derivatives and so on) and treatment (calibration, validation and prediction), so that a more reliable, general and robust prediction model can be established for a practical application.

Conclusions

An experimental set-up for PAS consisting of a PA accessory, tungsten bromine lamp, monochromator, chopper and lock-in-amplifier was successfully established. The PA signal was obtained, and the chopping frequency was optimised as 20 Hz using the model in the total spectral range of 800–2400 nm performed well. The predictions were excellent for SOM, acceptable for carbonate and Olsen P but relatively poor for clay. The primary advantage of the PAS approach, compared with conventional chemical methods, is the unique ability to directly predict SOM content as well as some other soil properties without soil sample pretreatment. This technique may provide an alternative option for rapid soil analysis.

Acknowledgements

This study was supported by the National Natural Science Foundation of China (41130749) and the National Fundamental Programme (973) (2015CB150403), and we thank Zolix Company (Beijing, China) for their valuable assistance in the experimental set-up of NIR-PAS. We are also very appreciative for the help from Dr Viscarra Rossel RA in recording the soil reflectance NIR spectra.

References

1. R.A. Viscarra Rossel, D.J.J. Walvoort, A.B. McBratney, L.J. Janik and J.O. Skjemstad, "Visible, near infrared, mid infrared or combined diffuse reflectance spectroscopy for simultaneous assessment of various soil properties", *Geoderma* **131**, 59 (2006). doi: <http://dx.doi.org/10.1016/j.geoderma.2005.03.007>
2. B. Kuang, H.S. Mahmood, M.Z. Quraishi, W.B. Hoogmoed, A.M. Mouazen and E.J. van Henten, "Sensing soil properties in the laboratory, in situ, and on-line. A review", *Adv. Agron.* **114**, 155 (2012). doi: <http://dx.doi.org/10.1016/B978-0-12-394275-3.00003-1>
3. S. Armenta, J. Moros, S. Garrigues and M. LaGuardia, "Direct determination of Mancozeb by photoacoustic spectroscopy", *Anal. Chim. Acta* **567**, 255 (2006). doi: <http://dx.doi.org/10.1016/j.aca.2006.03.031>
4. N.G.C. Astrath, A.C. Bento, M.L. Baesso, A. Ferreira da Silva and C. Persson, "Photoacoustic spectroscopy to determine the optical properties of thin film 4H-SiC", *Thin Solid Films* **515**, 2821 (2006). doi: <http://dx.doi.org/10.1016/j.tsf.2006.08.009>
5. J. Irudayaraj, H. Yang and S. Sakhamuri, "Differentiation and detection of microorganisms using Fourier transform infrared photoacoustic spectroscopy", *J. Mol. Struct.* **606**, 181 (2002). doi: [http://dx.doi.org/10.1016/S0022-2860\(01\)00869-9](http://dx.doi.org/10.1016/S0022-2860(01)00869-9)
6. J.G. Camilotti, A. Somer, G.F. Costa, M.A. Ribeiro, C. Bonardi, G.K. Cruz, S.L. Gomez, F.L. Beltrame, A.N. Medina, F. Sato, N.G.C. Astrath and A. Novatski, "The phase-resolved photoacoustic method indicate chemical assignments of paracetamol", *Spectrochim. Acta A* **121**, 719 (2014). doi: <http://dx.doi.org/10.1016/j.saa.2013.11.099>
7. C.W. Du and J.M. Zhou, "Application of infrared photoacoustic spectroscopy in soil analysis", *Appl. Spectrosc. Rev.* **46**, 405 (2011). doi: <http://dx.doi.org/10.1080/05704928.2011.570837>
8. C.W. Du, G.Q. Zhou, H.Y. Wang, X.Q. Chen and J.M. Zhou, "Depth profiling of clay-xanthan complexes using step-scan mid-infrared photoacoustic spectroscopy", *J. Soils Sed.* **10**, 855 (2010). doi: <http://dx.doi.org/10.1016/j.vib-spec.2008.04.009>
9. B. Zoltan, P. Andera and G.A. Szabo, "Photoacoustic instruments for practical applications: present, potentials, and future challenges", *Appl. Spectrosc. Rev.* **46**, 1 (2011). doi: <http://dx.doi.org/10.1080/05704928.2010.520178>
10. S. Kang, S. Kim, S. Kang, J. Lee, C.S. Cho, J.H. Sa and E.C. Jeon, "A study on N₂O measurement characteristics using photoacoustic spectroscopy (PAS)", *Sensors* **14**, 14399 (2014). doi: <http://dx.doi.org/10.3390/s140814399>
11. P. Marc and G. Jacques, *Handbook of Soil Analysis—Mineralogical, Organic and Inorganic Methods*. Springer-Verlag, Berlin, Germany. (2003).

12. R.K. Lu, *Agrochemical Analysis Methods in Soil Science*, China Agricultural Publisher, Beijing, China (1999).
13. A. Savitzky and M.J.E. Golay, "Smoothing and differentiation of data by simplified least squares procedures", *Anal. Chem.* **36**, 1627 (1964). doi: <http://dx.doi.org/10.1021/ac60214a047>
14. P. Geladi and B.R. Kowalski, "Partial least-squares regression: a tutorial", *Anal. Chim. Acta* **185**, 1 (1986).
15. V. Bellon-Maurel, E. Fernandez-Ahumada, B. Palagos, J. Roger and A. McBratney, "Critical review of chemometric indicators commonly used for assessing the quality of the prediction of soil attributes by NIR spectroscopy", *Trends Anal. Chem.* **29**, 1073 (2010). doi: <http://dx.doi.org/10.1016/j.trac.2010.05.006>
16. S. Pandhija, N.K. Rai, A.K. Singh, A.K. Rai and R. Gopal, "Development of photoacoustic spectroscopic technique for the study of materials", *Prog. Cryst. Growth Ch.* **52**, 53 (2006). doi: <http://dx.doi.org/10.1016/j.pcrysgrow.2006.03.022>
17. C.F. Zhou, W. Jiang, B.K. Via, O. Fasina and G.T. Han. "Prediction of mixed hardwood lignin and carbohydrate content using ATR-FTIR and FT-NIR", *Carbohydr. Polym.* **121**, 336 (2015). doi: <http://dx.doi.org/10.1016/j.carbpol.2014.11.062>
18. W. Kerstin, F. Karen, M.G. Alexander and P. Remigiusz, "Trends in near infrared spectroscopy and multivariate data analysis from an industrial perspective", *Proc. Eng.* **87**, 867 (2014). doi: <http://dx.doi.org/10.1016/j.proeng.2014.11.292>
19. J.M. Soriano-Disla, J. Janik, R.A. Viscarra Rossel, L.M. Macdonald and M.J. McLaughlin, "The performance of visible, near-, and mid-infrared reflectance spectroscopy for prediction of soil physical, chemical, and biological properties", *Appl. Spectrosc. Rev.* **49**, 139 (2014). doi: <http://dx.doi.org/10.1080/05704928.2013.811081>
20. J.G. Camilotti, A. Somer, G.F. Costa, M.A. Ribeiro, Bonardi, G.K. Cruz, S.L. Gómez, F.L. Beltrame, A.N. Medina and F. Sato, "The phase-resolved photoacoustic method to indicate chemical assignments of paracetamol", *Spectrochimica Acta Part A* **5**, 719 (2014). doi: <http://dx.doi.org/10.1016/j.saa.2013.11.099>
21. R.A. Viscarra Rossel and T. Behrens, "Using data mining to model and interpret soil diffuse reflectance spectra", *Geoderma* **158**, 46 (2010). doi: <http://dx.doi.org/10.1016/j.geoderma.2009.12.025>